Photoacoustics 20 (2020) 100198

Contents lists available at ScienceDirect

Photoacoustics

journal homepage: www.elsevier.com/locate/pacs

Research article

Synchronously Amplified Photoacoustic Image Recovery (SAPhIRe)

Aida A. Demissie[a,1], Donald VanderLaan[b,1], Md S. Islam[a], Stanislav Emelianov[b,c,**], Robert M. Dickson[a,*]

[a] School of Chemistry & Biochemistry, Georgia Institute of Technology, Atlanta, GA 30332, USA
[b] School of Electrical & Computer Engineering, Georgia Institute of Technology, Atlanta, GA 30332, USA
[c] Wallace H. Coulter Department of Biomedical Engineering, Georgia Institute of Technology and Emory University, Atlanta, GA 30332, USA

ARTICLE INFO

Keywords:
Modulation
Multimodal
Spectroscopy
Signal processing
Imaging
Fluorescence
Photoacoustics

ABSTRACT

In molecular and cellular photoacoustic imaging with exogenous contrast agents, image contrast is plagued by background resulting from endogenous absorbers in tissue. By using optically modulatable nanoparticles, we develop ultra-sensitive photoacoustic imaging by rejecting endogenous background signals and drastically improving signal contrast through time-delayed pump-probe pulsed laser illumination. Gated by prior pump excitation, modulatable photoacoustic (mPA) signals are recovered from unmodulatable background through simple, real-time image processing to yield background-free photoacoustic signal recovery within tissue mimicking phantoms and from ex-vivo tissues. Inherently multimodal, the fluorescence and mPA sensitivity improvements demonstrate the promise of Synchronously Amplified Photoacoustic Image Recovery (SAPhIRe) for PA imaging in diagnosis and therapy.

1. Introduction

There is a great need for the development of imaging and sensing technologies that can diagnose small, early stage pathologies deep within tissue. While a range of medical imaging modalities hold promise, none is perfect as many suffer from low sensitivity, poor resolution, high complexity/cost, or use of ionizing radiation. [1] Optical imaging and fluorescent labeling, in particular, have revolutionized cell biology, but direct imaging in deep tissue is limited by high optical scattering of both excitation and emission [2,3]. Conversely, less sensitive approaches such as ultrasound offer excellent penetration, but often poor contrast that relies on differences in mechanical properties within tissues. Combining optical excitation and acoustic detection, photoacoustic (PA) imaging is particularly promising, as optically generated acoustic waves are less susceptible to scattering and are readily detected with ultrasonic transducers [4–8]. Many endogenous agents such as blood produce strong photoacoustic signals, enabling natural contrast for imaging vasculature, but these and other natural absorbers simultaneously limit deep tissue and small pathology imaging, especially in the presence of blood.

PA signals result from pulsed optical excitation of strongly absorbing species that undergo efficient non-radiative decay [7,9]. Such rapid deposition of energy in the surrounding tissue generates an acoustic signal that can be detected with ultrasonic transducer arrays to image the location of optical contrast agent. While strongly absorbing dyes such as methylene blue and indocyanine green have been used to label and recover PA signals from sentinel lymph nodes, for example [10–12], high dye concentrations must be achieved at the site of the pathology of interest so that multispectral or other photoacoustic imaging approaches can be used to visualize signals in the presence of high background, in vivo. To circumvent the need for high injected dye concentrations and to provide potential targeting opportunities, non-degradable noble-metal nanoparticles and carbon nanotubes have been explored as PA contrast agents [5,13–19]. Whether using high concentration dyes or nanoparticles as contrast agents, both acute and long-term toxicity concerns need to be addressed [20–22], as only rarely are these particles clearable [23].

Although stronger signals are always beneficial, background suppression can even more drastically improve sensitivity to smaller and deeper pathologies in both biological and medical imaging. Initially demonstrated in fluorescence imaging [24–27], dual-laser mediated background suppression techniques using molecule-specific dark state populations, drastically improve imaging sensitivity and offer promise for multimodal detection in high background. Recently applied to PA

* Corresponding author.
** Corresponding author at: School of Electrical & Computer Engineering, Georgia Institute of Technology, Atlanta, GA 30332, USA.
E-mail addresses: stas@gatech.edu (S. Emelianov), dickson@chemistry.gatech.edu (R.M. Dickson).
[1] These authors contributed equally to this work.

https://doi.org/10.1016/j.pacs.2020.100198
Received 26 March 2020; Received in revised form 22 June 2020; Accepted 29 June 2020
Available online 01 July 2020

detection using heavily averaged pulse trains from non-emissive methylene blue [28] and voxel-by-voxel stimulated emission depletion [25] from strong fluorophores in phantoms [29,30], modulated PA detection has been demonstrated, but to date has required saturating intensities and long acquisition times. Herein, we develop and utilize the first optically modulatable multimodal contrast agent – rose bengal-doped silica nanoparticles for drastically improved contrast in PA signal recovery from two laser pulses with images being directly acquired with array detectors. Such rapid image acquisition benefits from the vast sensitivity improvement rose bengal offers in fluorescence detection [24]. While various nanoparticle/dye formulations are feasible, the high charge on rose bengal makes silica nanoparticles an excellent vehicle to obtain high dye concentrations and biodegradability [31]. Most importantly, rose bengal-doped silica nanoparticles completely suppress photoacoustic signal from blood and background tissue to directly recover modulated photoacoustic (mPA) signals from nanoparticles within whole blood and deep within tissue, in near real time.

Highly successful in suppressing background in fluorescence imaging, Synchronously Amplified Fluorescence Image Recovery (SAFIRe) utilizes pump and probe excitations to modulate ground and intermediate state populations [24,32,33]. Because intermediate states have lifetimes of at least several microseconds and have distinct absorption spectra, the pump laser prepares the intermediate state population while the delayed, long-wavelength probe laser excites the prepared intermediate state to regenerate the ground state of the fluorescent manifold, thereby dynamically increasing fluorescence. Because such optical gating of fluorescence results from optically controlling the ground and intermediate state dye populations, optical contrast in photoacoustic imaging can be analogously produced, with long-wavelength secondary-induced PA signals arising only if preceded by pump laser excitation. Thus, the same pump-probe process should enable Synchronously Amplified Photoacoustic Image Recovery (SAPhIRe) to remove all non-gated PA signals of endogenous chromophores and to produce background free PA images.

While all photoacoustic contrast agents, endogenous or exogenous, strongly absorb pump laser excitation from their ground states with rapid non-radiative relaxation, optically modulatable (OM) PA dyes instead efficiently generate long-lived intermediate states that can be subsequently excited at a longer wavelength. Although endogenous chromophores generate PA signals from both pump and probe excitations [34], their probe-excited PA signals are independent of prior pump excitation. Modulatable dye PA signals from probe excitation, however, must be optically gated by prior pump excitation to first produce long-lived intermediate states. It is these long-lived states that absorb and produce PA signals under subsequent long-wavelength excitation, but not without prior pump excitation to prepare the intermediate state. Thus, because mPA signals are only generated when probe excitation is gated by pump excitation, operationally, mPA signals should follow the logic: ((IF pump) AND probe). PA signal from blood, however, follows the logic of (pump OR probe). This linearity in blood signals enables subtraction of blood PA background from the nonlinear pump + probe images to yield background-suppressed mPA contrast (Fig. 1).

2. Results and discussion

2.1. Modulatable RB-SiO_2-NP synthesis and characterization

To create modulatable photoacoustic (mPA) contrast agents for detection in blood-laden background, we increased local modulatable dye concentration through rose bengal (RB) incorporation in (biodegradable) ~100-nm silica nanoparticles, using a capped mesoporous silica synthesis [35]. Briefly, 200 mg of CTAB (cetyl trimethyl ammonium bromide) was dissolved in 95 mL of DI water. 0.8 mL of RB (5 mg/mL) and 0.7 mL of 2 M sodium hydroxide were added to the solution. The reaction was heated to 80 °C and allowed to stabilize for ~1 h, after which 1 mL of TEOS was added under constant stirring. After 2 h, another 1 mL aliquot of TEOS was added dropwise to limit formation of additional silica seeds. The reaction was allowed to proceed for another hour. Particles were centrifuged and washed three times to remove unreacted dye and suspended in water. Rose bengal-doped silica nanoparticle (RB-SiO_2-NP) size was confirmed via TEM (Fig. 2a). UV–vis measurements of RB absorption coupled with measured nanoparticle particle densities reveal a per-particle RB concentration of ~5 mM. Upon absorption at 532 nm, rose bengal efficiently populates its triplet state with a > 90 % quantum yield and weak fluorescence. As both fluorescence modulation and PA modulation rely on optically controlling intermediate state populations, modulated particle fluorescence was characterized optically as a surrogate for initial photoacoustic response. RB-SiO_2-NP optical modulation was performed with pulsed 532 nm pump excitation to prepare the intermediate state, followed by continuous wave 830 nm (probe) that excites the lowest lying triplet (intermediate state, T_1, see Fig. 1) to excited triplet states with some small fraction of reverse intersystem crossing (RISC) to regenerate the emissive singlet state. While the majority of triplet-triplet excitations decay nonradiatively to repopulate T_1, this probe process produces a small amount of optically activated delayed fluorescence (OADF) at ~590 nm that is readily detected [36]. Modulation depth, defined as the normalized difference in fluorescence with both pump and probe relative to that generated by pump alone (no fluorescence is observed with probe only), was measured to be ~40 %. The OADF decay (Fig. 2b) is a direct measurement of the intermediate state lifetime, and for RB-SiO_2-NPs this lifetime is ~20 μs – long enough to measure the optically gated probe PA signal while temporally separating it from the pump-induced PA signal. Longer pump-probe delays generate SAPhIRe signals that are reduced similarly to fluorescence decay shown in Fig. 2b, with the largest SAPhIRe signal resulting from the shortest possible distinguishable pump-probe delay. Because pump-only and probe-only signals are subtracted from the nonlinear pump + probe signal, background-free SAPhIRe from mPA nanoparticles can be performed at short, ~200 ns delays to simultaneously maximize modulated photoacoustic signal and reject photoacoustic background signal.

2.2. Modulated PA signal recovery from RB-SiO_2-NPs within whole blood

Pulsed pump excitation at 532 nm (~10 ns, 10 mJ/cm^2 per pulse) generates strong PA signals from both blood and RB-SiO_2-NPs. Pulsed probe excitation at 1064 nm (~10 ns, 10 mJ/cm^2 per pulse) also generates PA signals from blood, but no PA signals from RB-SiO_2-NPs are produced unless it is pre-illuminated at 532 nm. Such optical preparation of the intermediate state enables simple subtraction of 1064 nm generated signals with and without 532 nm pre-illumination to selectively recover PA signals from RB-SiO_2-NPs (Fig. 1). To assay detection of RB-SiO_2-NPs via photoacoustic imaging (SAPhIRe), we constructed tissue mimicking phantoms with several inclusions. The bulk material was composed of tissue-mimicking synthetic rubber (Hummic Medical #5 gel) mixed with 2 % silica powder to provide ultrasound scattering. Within the larger phantom body were placed three cylindrical inclusions – one containing only RB-SiO_2-NPs, another one red blood cells only, and the third inclusion containing mixture of red blood cells and RB-SiO_2-NPs. The inclusions were constructed by using tissue mimicking alginate in which nanoparticle suspensions and/or red blood cells were mixed with 10 %wt sodium alginate solution in a 1:1 vol ratio and poured into a template. Crosslinking occurs by submerging the templated solution in a calcium-containing aqueous solution ($CaCl_2$) for 10 min, after which the template can be removed and physically inserted into the larger bulk synthetic tissue phantom. Phantom (Fig. 3A) was imaged using ultrasound (US) and photoacoustic imaging system based on a research-grade commercial ultrasound imaging system (Vantage 128, Verasonics, Inc.) interfaced with two nanosecond pulsed Nd:YAG lasers operating at 532 nm and 1064 nm wavelengths (Tempest and Gemini PIV, both from New Wave

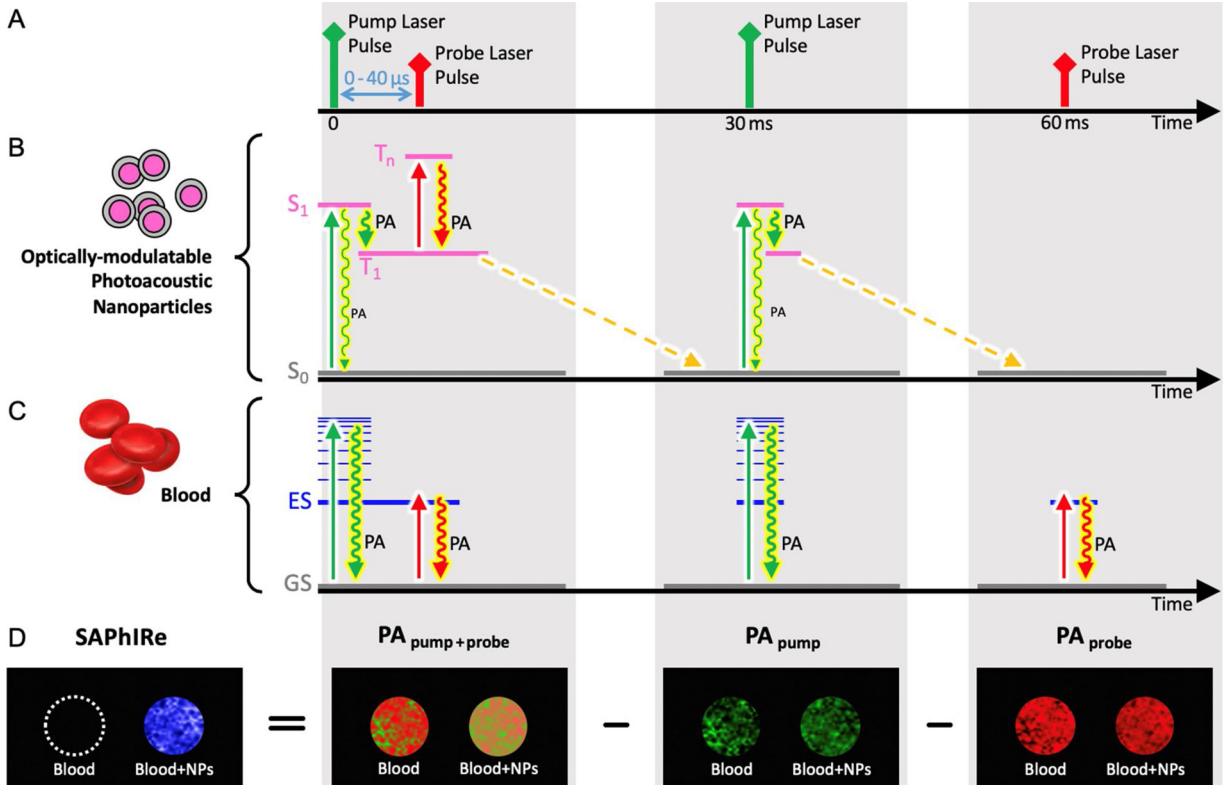

Fig. 1. SAPhIRe imaging paradigm. The diagram illustrates the different photophysical states affected by (A) pump laser pulse (532 nm, green) and probe laser pulse (1064 nm, red) in (B) optically modulatable photoacoustic (mPA) contrast agents versus (C) blood. The imaging sequence consisting of pump-probe, pump, and probe laser pulses results in (D) PA images that can be acquired and processed to produce background-free PA images of optically modulatable nanoparticles within tissue.

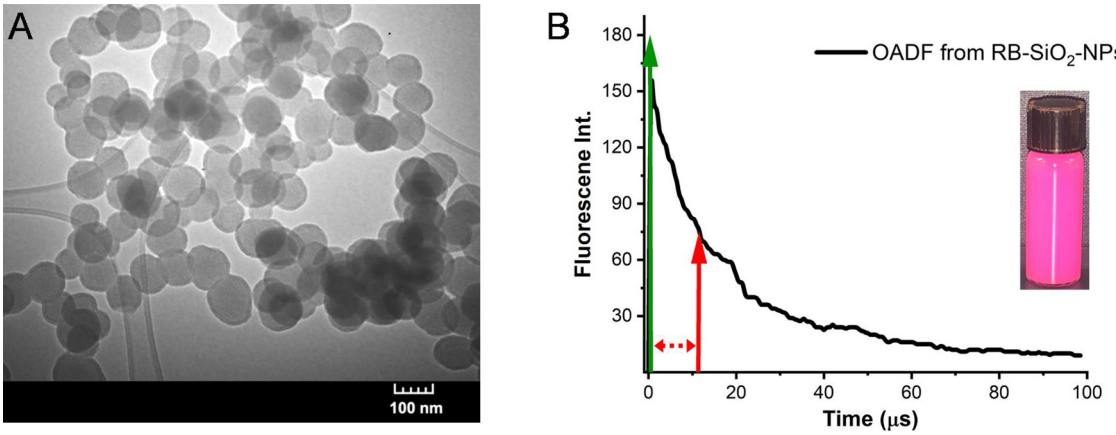

Fig. 2. (A) TEM image of as synthesized rose bengal loaded silica nanoparticles, RB-SiO_2-NPs (diameter = 95 ± 14 nm). (B) OADF decay of RB-SiO_2-NPs upon probe illumination with green arrow indicating time of pump pulse and red arrow showing the probe pulse after user-controlled delay. Exponential fit of the OADF decay indicates an intermediate state lifetime of ~20 µs.

Research). An ultrasound transducer array operating at 8 MHz center frequency was used for ultrasound B-scan imaging (Fig. 3B) and to record PA signals. For PA imaging, the two optical beams from two lasers were spatially combined on a dichroic mirror and passed through a diffuser before impinging on the phantom, which was submerged in a water tank to provide ultrasonic coupling with the ultrasound transducer. Optical illumination was normal to the US imaging plane (Fig. 3B). Software was written to perform image subtraction and SAPhIRe image recovery in real time, allowing for SAPhIRe images to be rendered live within 100 ms for 30 Hz laser excitation. Three photoacoustic image acquisitions were needed to construct the final SAPhIRe image: 1) PA image from combined pump (532 nm) and probe (1064 nm) illumination (Fig. 3D), 2) PA image from pump (532 nm) illumination only (Fig. 3E), and 3) PA image from only probe (1064 nm) illumination (Fig. 3F). The SAPhIRe data (Fig. 3C) was generated by subtracting both the pump-only PA and the probe-only PA from the pump + probe PA dataset. Although the dark-state lifetime for RB-SiO_2-NPs is sufficiently long to delay pump and probe illuminations such that only two acquisitions are necessary, SAPhIRe signals were generally larger by minimizing the delay between pump and probe excitations. Thus, the actual delay used between pump and probe was ~200 ns. As evident from Fig. 3, the inclusion with RB-SiO_2-NPs generates no 1064 nm-only induced PA signals. When primed by a 532 nm laser pulse, however, the large laser-induced intermediate state population responds strongly to the subsequent 1064 nm laser pulse (i.e. (IF 532 nm) AND 1064 nm). The blood inclusion responds identically to

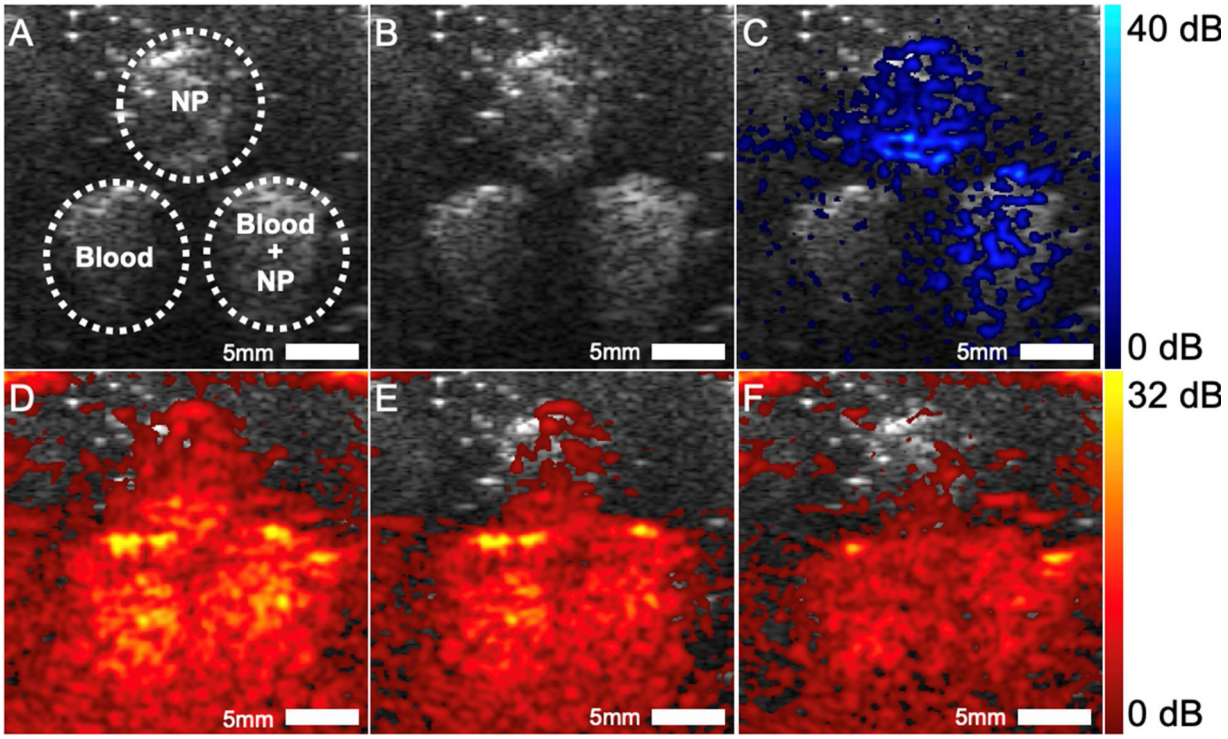

Fig. 3. SAPhIRe from blood-laden phantoms. (A) Phantom geometry: top inclusion contains RB-SiO_2-NPs, lower left inclusion contains 10 % blood, and lower right inclusion contains mixture of 10 % blood and RB-SiO_2-NPs. B) Ultrasound image of phantom. (B) Ultrasound image of the phantom. (C) SAPhIRe image showing suppression of background (i.e., blood) signal. (D) PA image taken with 532 nm pump and 1064 nm probe illumination. (E) PA image taken with pump illumination only, overlaid on US. (F) PA image taken with probe illumination only. Dynamic range for US, PA, and SAPhIRe images is 40, 32, 40 dB respectively, with below-range values mapped transparently for color data. The SAPhIRe dynamic range is intentionally increased over that in the PA component images to show the noise floor and the lack of signal from blood alone.

the 1064 nm irradiation regardless of initial excitation by 532 nm (i.e. 532 nm OR 1064 nm), enabling direct subtraction of pump-induced and probe-induced PA images from pump + probe-induced PA images to nearly perfectly eliminate PA signals from red blood cells while retaining the signal from optically modulatable RB-SiO_2-NPs. Thus, the hemoglobin in blood cells also serves as a control showing that SAPhIRe signals are only observed with specific mPA contrast agents.

2.3. SAPhIRe contrast from within muscle tissue

To demonstrate the potential of SAPhIRe, even while using poorly penetrating 532 nm pump laser light, ex vivo small animal imaging experiment was performed. We intramuscularly injected 50 μL of aqueous or glycerol solutions of RB-SiO_2-NPs into the left hamstrings of a rat. Hair was removed but skin was intact. Rodent was illuminated and imaged from opposite sides, with the US transducer lateral and the optical excitation impinging on the medial surface. The bolus was injected at an approximate depth of 9 mm, the same distance that the light had to traverse to reach it. Because RB-SiO_2-NPs are fluorescent, the location of bolus injection is clearly discernable via fluorescence (Fig. 4A) confirming the injection. As expected, ultrasound image (Fig. 4B), rendered with logarithmic compression and displayed using 40 dB dynamic range, shows the anatomical landmarks of the imaged tissue but cannot reliably distinguish the injected bolus of RB-SiO_2-NPs. In contrast, photoacoustic SAPhIRe image (Fig. 4C, 32 dB dynamic range with below-range signals mapped transparently for color data) clearly show the location of RB-SiO_2-NPs. Strong PA signals dominate the component images (Fig. 4D–F, 32 dB) where the light enters the tissue, as expected with intact skin, and from red blood cells within the tissue. Despite the strong subsurface fluence effects and PA signals from tissue, the bolus injection is readily apparent in the composite SAPhIRe image, as background PA is nearly completely suppressed. The injection trajectory, from the US image perspective, was directed upward, arriving from below – so expected trace signal is observed in SAPhIRe from contrast agent that leaked out through the injection tract. PA signal is absent on the left sides of PA images in Fig. 4D–F as this region was not illuminated with either laser beams. As SAPhIRe sensitivity gains result from background rejection, we estimate ~20-fold improvement in signal visibility over conventional PA imaging, consistent with fluorescence modulation signal gains. [26] Further, although detection limits are difficult to estimate without targeting, imaging the injected 50 μL RB@SiO_2 NP solution (6.8×10^{13} NPs/mL, 7 mM RB/NP, ~95 nm diameter) resulted in a sufficiently high SAPhIRe signal contrast that we expect to be able to decrease injected contrast agent levels by at least 280-fold without lowering the detection window floor.

Despite very strong contrast, the optical fluences employed were far below ANSI limits. The incident 532 nm pump radiation was 3 mJ/cm^2, while the 1064 nm probe fluence was 7 mJ/cm^2. This implies we would have been able to successfully detect far lower concentrations of particles, because, the signal strength here is already very high, and if needed, we are able to increase the laser intensity by a factor of ~7 and ~15 before exceeding ANSI limits [37].

3. Conclusion

Modulated photoacoustic excitation of optically modulatable nanoparticles enables deep-penetrating, high contrast and sensitivity, background-free photoacoustic imaging. We have presented a real time background rejection paradigm for PA imaging with significant signal enhancements over background. Compared with standard single-laser photoacoustic detection, endogenous chromophore signals and subsurface fluence effects are entirely suppressed. Although spectroscopic PA can achieve this, in practice the number of PA acquisitions required for spectral unmixing can be problematic regarding motion artifacts

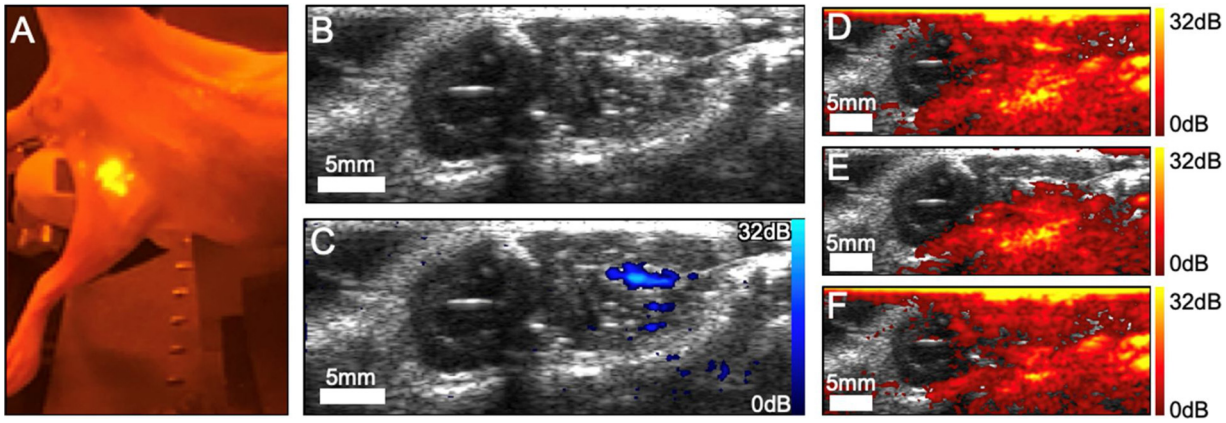

Fig. 4. Ex vivo imaging results. A) Fluorescent image of animal with bolus injection of RB-SiO_2-NPs. B) Post-injection ultrasound image (40 dB). Retrospectively, the bolus is visible as an oblong hyperechoic region. C) SAPhIRe overlay (32 dB): the bolus (hyperechoic US region) and SAPhIRe signal spatially overlap. SAPhIRe signal is also present along the trajectory of the injection needle introduced from the bottom. Illumination traversed approximately 9 mm of tissue to reach the bolus. D) PA overlay using both pump and probe excitations. E) PA overlay using pump excitation. F) PA overlay using probe excitation. All PA images are displayed using 32 dB dynamic range. The US, SAPhIRe and PA images are 16 mm by 38 mm.

and background and contrast agent signals should be of similar strengths. SAPhIRe achieves nearly complete suppression of unwanted signal with only two wavelengths and three RF acquisitions. RB-SiO_2-NPs not only allow for background suppression in photoacoustic imaging but also offer a path to a dual imaging modality of modulated photoacoustic and fluorescence imaging (SAFIRe). Further SAPhIRe/SAFIRe techniques can be used to distinguish among several probes simultaneously based on dark state lifetimes and mapping time decays of modulatable PA and fluorescence signatures.

Declaration of Competing Interest

The authors declare that there are no conflicts of interest.

Acknowledgments

We would like to thank N. Wu from Peking University and V.S. Jisha and S. Sarkar of the Georgia Institute of Technology for helpful discussions. The work was supported in part by the Vasser Woolley Foundation, National Institutes of Health under grants CA158598 and EB028916, and the Breast Cancer Research Foundation under grant BCRF-19-043.

References

[1] L.V. Wang, H. Wu, Biomedical Optics Principles and Imaging, Wiley and Sons, Inc, New Jersey, 2007.
[2] K. Elgass, K. Caesar, D. Wanke, K. Harter, A. Meixner, F. Schleifenbaum, Application of FLIM-FIDSAM for the in vivo analysis of hormone competence of different cell types, Anal. Bioanal. Chem. 398 (5) (2010) 1919–1925.
[3] Y. Sun, J. Phipps, D.S. Elson, H. Stoy, S. Tinling, J. Meier, B. Poirier, F.S. Chuang, D.G. Farwell, L. Marcu, Fluorescence lifetime imaging microscopy: in vivo application to diagnosis of oral carcinoma, Opt. Lett. 34 (13) (2009) 2081–2083.
[4] C. Kim, T.N. Erpelding, L. Jankovic, M.D. Pashley, L.V. Wang, Deeply penetrating in vivo photoacoustic imaging using a clinical ultrasound array system, Biomed. Opt. Express 1 (1) (2010) 278–284.
[5] G. Luke, D. Yeager, S. Emelianov, Biomedical applications of photoacoustic imaging with exogenous contrast agents, Ann. Biomed. Eng. 40 (2) (2012) 422–437.
[6] K. Maslov, H.F. Zhang, S. Hu, L.V. Wang, Optical-resolution photoacoustic microscopy for in vivo imaging of single capillaries, Opt. Lett. 33 (9) (2008) 929–931.
[7] L. Wang, Photoacoustic Imaging and Spectroscopy Vol. 144 CRC Press, 2009.
[8] L.V. Wang, S. Hu, Photoacoustic tomography: in vivo imaging from organelles to organs, Science 335 (6075) (2012) 1458–1462.
[9] L.V. Wang, Prospects of photoacoustic tomography, Med. Phys. 35 (12) (2008) 5758–5767.
[10] K.H. Song, E.W. Stein, J.A. Margenthaler, L.V. Wang, Noninvasive photoacoustic identification of sentinel lymph nodes containing methylene blue in vivo in a rat model, J. Biomed. Opt. 13 (5) (2008) 054033.
[11] T.N. Erpelding, C. Kim, M. Pramanik, L. Jankovic, K. Maslov, Z. Guo, J.A. Margenthaler, M.D. Pashley, L.V. Wang, Sentinel lymph nodes in the rat: noninvasive photoacoustic and US imaging with a clinical US system, Radiology 256 (1) (2010) 102–110.
[12] C. Kim, K.H. Song, F. Gao, L.V. Wang, Sentinel lymph nodes and lymphatic vessels: noninvasive dual-modality in vivo mapping by using indocyanine green in rats–volumetric spectroscopic photoacoustic imaging and planar fluorescence imaging, Radiology 255 (2) (2010) 442–450.
[13] A. de la Zerda, S. Bodapati, R. Teed, S.Y. May, S.M. Tabakman, Z. Liu, B.T. Khuri-Yakub, X. Chen, H. Dai, S.S. Gambhir, Family of enhanced photoacoustic imaging agents for high-sensitivity and multiplexing studies in living mice, ACS Nano 6 (6) (2012) 4694–4701.
[14] A. De La Zerda, C. Zavaleta, S. Keren, S. Vaithilingam, S. Bodapati, Z. Liu, J. Levi, B.R. Smith, T.-J. Ma, O. Oralkan, Z. Cheng, X. Chen, H. Dai, B.T. Khuri-Yakub, S.S. Gambhir, Carbon nanotubes as photoacoustic molecular imaging agents in living mice, Nat Nano 3 (9) (2008) 557–562.
[15] K.A. Homan, M. Souza, R. Truby, G.P. Luke, C. Green, E. Vreeland, S. Emelianov, Silver nanoplate contrast agents for in vivo molecular photoacoustic imaging, ACS Nano 6 (1) (2011) 641–650.
[16] J.-W. Kim, E.I. Galanzha, E.V. Shashkov, H.-M. Moon, V.P. Zharov, Golden carbon nanotubes as multimodal photoacoustic and photothermal high-contrast molecular agents, Nat Nano 4 (10) (2009) 688–694.
[17] S. Mallidi, T. Larson, J. Tam, P.P. Joshi, A. Karpiouk, K. Sokolov, S. Emelianov, Multiwavelength photoacoustic imaging and Plasmon resonance coupling of gold nanoparticles for selective detection of cancer, Nano Lett. 9 (8) (2009) 2825–2831.
[18] L. Pai-Chi, C.W. Wei, C.K. Liao, C.D. Chen, K.C. Pao, C.R.C. Wang, Y.N. Wu, D.B. Shieh, Photoacoustic imaging of multiple targets using gold nanorods, IEEE Trans. Ultrason. Ferroelectr. Freq. Control 54 (8) (2007) 1642–1647.
[19] Q. Zhang, N. Iwakuma, P. Sharma, B.M. Moudgil, S.R. Grobmyer, H. Jiang, In Vivo Photoacoustic Imaging of Tumor Using Gold Nanoparticles As Contrast Agent, Biomedical Optics and 3-D Imaging, Miami, Florida, 2010/04/11, Optical Society of America, Miami, Florida, 2010 p BTuD23.
[20] C. Cheng, K.H. Muller, K.K.K. Koziol, J.N. Skepper, P.A. Midgley, M.E. Welland, A.E. Porter, Toxicity and imaging of multi-walled carbon nanotubes in human macrophage cells, Biomaterials 30 (25) (2009) 4152–4160.
[21] D.X. Cui, F.R. Tian, C.S. Ozkan, M. Wang, H.J. Gao, Effect of single wall carbon nanotubes on human HEK293 cells, Toxicol. Lett. 155 (1) (2005) 73–85.
[22] Z. Liu, C. Davis, W. Cai, L. He, X. Chen, H. Dai, Circulation and long-term fate of functionalized, biocompatible single-walled carbon nanotubes in mice probed by Raman spectroscopy, Proc. Natl. Acad. Sci. 105 (5) (2008) 1410–1415.
[23] X. Jiang, B. Du, S. Tang, J.-T. Hsieh, J. Zheng, Photoacoustic imaging of nanoparticle transport in the kidneys at high temporal resolution, Angew. Chem. Int. Ed. Engl. 58 (18) (2019) 5994–6000.
[24] C.I. Richards, J.-C. Hsiang, R.M. Dickson, Synchronously amplified fluorescence image recovery (SAFIRe), J. Phys. Chem. B 114 (2010) 660–665.
[25] C. Fan, J.-C. Hsiang, A.E. Jablonski, R.M. Dickson, All-optical fluorescence image recovery using modulated stimulated emission depletion, Chem. Sci. 2 (6) (2011) 1080–1085.
[26] J.-C. Hsiang, A.E. Jablonski, R.M. Dickson, Optically modulated fluorescence bioimaging: visualizing obscured fluorophores in high background, Acc. Chem. Res. 47 (5) (2014) 1545–1554.
[27] S. Sarkar, C. Fan, J.-C. Hsiang, R.M. Dickson, Modulated fluorophore signal recovery buried within tissue mimicking phantoms, J. Phys. Chem. A 117 (39) (2013) 9501–9509.
[28] J.W.Y. Tan, C.H. Lee, R. Kopelman, X. Wang, Transient triplet differential (TTD) method for background free photoacoustic imaging, Sci. Rep. 8 (1) (2018) 9290.
[29] J. Märk, F.-J. Schmitt, C. Theiss, H. Dortay, T. Friedrich, J. Laufer, Photoacoustic imaging of fluorophores using pump-probe excitation, Biomed. Opt. Express 6 (7) (2015) 2522–2535.
[30] J. Märk, A. Wagener, E. Zhang, J. Laufer, Photoacoustic pump-probe tomography of

fluorophores in vivo using interleaved image acquisition for motion suppression, Sci. Rep. 7 (1) (2017) 40496.
[31] S.-A. Yang, S. Choi, S.M. Jeon, J. Yu, Silica nanoparticle stability in biological media revisited, Sci. Rep. 8 (1) (2018) 185.
[32] C. Fan, J.-C. Hsiang, R.M. Dickson, Optical modulation and selective recovery of Cy5 fluorescence, ChemPhysChem 13 (4) (2012) 1023–1029.
[33] C.I. Richards, J.-C. Hsiang, D. Senapati, S. Patel, J. Yu, T. Vosch, R.M. Dickson, Optically modulated fluorophores for selective fluorescence signal recovery, J. Am. Chem. Soc. 131 (13) (2009) 4619–4621.
[34] Y. Zhang, H. Hong, W. Cai, Photoacoustic imaging, Cold Spring Harb. Protoc. 2011 (9) (2011), https://doi.org/10.1101/pdb.top065508pdb.top065508.
[35] A. Yildirim, M. Turkaydin, B. Garipcan, M. Bayindir, Cytotoxicity of multifunctional surfactant containing capped mesoporous silica nanoparticles, RSC Adv. 6 (38) (2016) 32060–32069.
[36] A.A. Demissie, R.M. Dickson, Triplet shelving in fluorescein and its derivatives provides delayed, background-free fluorescence detection, J. Phys. Chem. B (2019) Submitted.
[37] American National Standard for safe use of lasers (ANSI 136.1) The Laser Institute of America 2007.

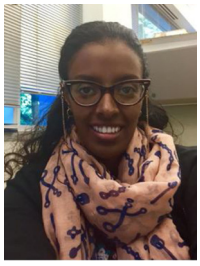

Dr. Aida Demissie received her undergraduate degree in chemistry from Jackson State University in 2012 and earned her graduate degree in Chemistry in 2019 from the Georgia Institute of Technology. As a graduate fellow she has worked in Dr. Robert Dickson's lab developing novel, non-invasive, acoustic and/or optical bio imaging techniques used to improve tumor visualization over obscuring background signals. She is currently employed as a consultant in the life sciences division of Simon - Kucher & Partners in Chicago, IL.

Don VanderLaan is currently a research engineer in the department of Electrical & Computer Engineering at Georgia Institute of Technology, Atlanta GA. His interests include cardiovascular disease, ultrasound and photoacoustic imaging, medical devices, imaging system design, and experiment automation. Don earned his B.S. in Electrical Engineering at Michigan State University in 2009.

Md Shariful Islam is a PhD student in chemistry and biochemistry at the Georgia Institute of Technology working under the supervision of Dr. Robert Dickson. He received his undergraduate and Master's degrees in chemistry in 2010 and 2012 from University of Dhaka, Bangladesh. Currently, his research focused on synthesis and characterization of modulable dye nanoparticles for non-invasive cancer/tumor detection using photoacoustic imaging.

Dr. Stanislav Emelianov is a Joseph M. Pettit Endowed Chair, Georgia Research Alliance Eminent Scholar, and Professor of Electrical & Computer Engineering and Biomedical Engineering at the Georgia Institute of Technology and Emory University School of Medicine. Dr. Emelianov is also the Director of the Ultrasound Imaging and Therapeutics Research Laboratory. Projects in Dr. Emelianov's laboratory are focused on the discovery, development, and clinical translation of diagnostic imaging and therapeutic instrumentation, augmented with theranostic nanoagents.

Dr. Robert Dickson is the Vasser Woolley Professor of Chemistry at Georgia Tech. He earned undergraduate and graduate degrees from Haverford College and The University of Chicago, respectively. After postdoctoral work at UCSD, he joined Georgia Tech's faculty in 1998, where he has pioneered the development and use of optically modulatable contrast agents to selectively recover weak signals buried within high background. Current efforts in his lab involve the development of chromophores and tailored application of modulation-based signal recovery to spy on biologically relevant processes in their native environments and statistical and optical methods for rapid antibiotic susceptibility testing from infected blood.